DEVELOPMENT OF COIR, GLASS FIBER AND SiC-REINFORCED EPOXY RESIN HYBRID COMPOSITES FOR BUILDING PANELS APPLICATIONS

R. GOPAL,[*] K. ANANTHAKUMAR,[**] T. ARUN NELLAIAPPAN,[***]
R. PADMESH[****] and E. ARUN[*****]

[*]*Department of Mechanical Engineering, Trichy Engineering College, India*
[**]*Process Engineering Department, Motherson Health and Medical System, Kanchipuram, India*
[***]*Department of Mechanical Engineering, SRM-TRP Engineering College, India*
[****]*Department of Mechanical Engineering, Amrita School of Engineering, Amrita Vishwa Vidhyapeetham, India*
[*****]*Department of Mechanical Engineering, Karpagam College of Engineering, Coimbatore-032, India*
✉ *Corresponding author: K. Anantha Kumar, Ananthakumar.kasi@motherson.com*

Received February 2, 2024

In this paper, hybrid composites were fabricated by incorporating coir fiber, glass fiber, and silicon carbide (SiC) into an epoxy resin matrix. The composites were developed to assess tensile, flexural, and impact properties, adhering to ASTM standards. Among the samples, the composite containing proportions of 20% coir and 20% glass fiber, along with 10% SiC, exhibited the highest tensile strength of approximately 100 MPa, flexural strength of 146 MPa, and impact strength of 85.4 kJ/m². Additionally, this sample demonstrated a water absorption rate of just 8%. Thermal gravimetric analysis revealed that composites with varying coir ratio, such as 10%, 20%, 30% and 40% coir reinforced with SiC, showed enhanced thermal stability, particularly due to the lignin present in coir fiber. The XRD and FTIR analyses confirmed the presence of coir, glass fiber, and SiC within the composites. These findings suggest that the proposed hybrid composites offer potential for applications in the building industry, such as exterior walls, indoor panels and floor tiles.

Keywords: hybrid composites, construction panels, mechanical properties, FTIR analysis, XRD analysis, coir, glass fiber

INTRODUCTION

Fiber reinforced composites (FRCs) are widely used in the energy, automotive and aerospace industries, among others, due to their strength, lightweight design, crashworthiness, corrosion resistance, and fatigue resistance.[1-3] Industries and technologies are increasingly seeking eco-friendly materials with improved properties. Natural fibers (NFs), such as coir, jute, kenaf, sisal, flax, and bamboo leaf fibers, are popular for making composites due to their low density, biodegradability, and recyclability, as well as reasonable strength.[5-7] However, synthetic fibers are often preferred due to their higher strength. To overcome this, researchers have combined two or more different natural fibers in a matrix, resulting in improved strength that challenges synthetic FRCs.[4]

Coir, extracted from the husk of the coconut fruit, is one such fiber with fair strength and durability. Coir is composed of 36-43% cellulose, 32.25% lignin and 15.17% hemicelluloses.[9] Coir has high strength, high elongation, low density (1.1-1.5 g/cm^3), and elastic modulus comparable to that of other natural fibers.[10-11] It also has a low rate of degradation due to its high lignin content.[12-13] The tensile strength of coir ranges from 105-593 MPa, with a Young's modulus of 2-8 GPa.[11] Coir was initially used in biodegradable fabrics for erosion control and seats.[14-15] Coir FRCs can be fabricated through various methods, such as injection molding, resin transfer molding, open molding, and compression molding. Compression molding has many benefits over other methods, including the ability to handle more fibers at high pressure and

temperature, resulting in better dimensional stability, fair thermo-mechanical properties, and uniform density.[16] When coir has a lower amount of hemicelluloses and cellulose, it tends to have lower stiffness and tensile strength.[16] However, if foreign particles are present in the composite, this can lead to poor bonding between the polymer and fiber.[17-19] Coir fiber contains a polarized hydroxyl group (OH), which is common among lignocellulosic fibers.[20] Additionally, coir is hydrophilic, and absorbs moisture from the atmosphere, resulting in a weak bond between natural fiber and a polymer matrix. This limits its application to dry environments.[11]

To improve interfacial bonding through surface modification, researchers have utilized various methods, such as the alkaline treatment, plasma treatment, enzymatic treatment and saline modification. Among these methods, the alkaline treatment is the most effective.[11,21,22] This is because it removes impurities, such as oil and wax, from the fiber surface and creates a rough surface that enhances good bonding, resulting in superior mechanical behavior.[23]

Modern construction panels and gutters are commonly made from composites, such as glass fiber reinforced polymer composites (GFRPs).[24-30] GFRPs are preferred over traditional steel materials due to their lighter weight, increased strength, stiffness, high resistance to corrosion, and ease of repair and fabrication.[31-33] The properties of GFRPs can be adjusted by using different types of fibers, changing their orientation, and adjusting the volume fraction used.[34] The number of fibers used, the quality of the fibers, the adhesion of composite constituents, and bonding between interfaces all affect the behavior of fiber composites.[35-37] Recently, researchers have focused on hybrid composites that use two or more different fibers in a matrix to meet dynamic property requirements. The properties of natural fiber-reinforced composites (NFRCs) can also be influenced by using multiple fibers, treating fibers to alter surface properties, using filler materials, and choosing the appropriate matrix.[38-39] Hybridization with sisal fiber notably improved the mechanical properties of SGF/SiC/Epoxy composite, and the addition of 10% SiC as a filler improved the composite's hardness and reduced its water-absorbing capacity.[40]

There have been numerous studies on the hybridization of natural fiber composites, which have resulted in improved mechanical properties, thermal properties, and water absorption properties. However, after conducting a thorough literature review, it was found that research on natural and synthetic fiber-reinforced composites is limited because of challenges like weak interfacial bonding between hydrophilic natural fibers and hydrophobic synthetic fibers, moisture absorption by natural fibers, and durability concerns. Natural fibers degrade faster and absorb moisture, affecting long-term performance. Combining these fibers in a matrix also presents manufacturing complexities, limiting such research. The novelty of this study consists in combining coir and glass fibers with a SiC filler, using NaOH treatment of natural fiber to improve bonding. It comprehensively evaluates mechanical and thermal properties, and offers a sustainable approach to creating high-performance hybrid composites for construction applications.

EXPERIMENTAL

Materials

The coir used to fabricate the composite was prepared manually from dried matured coconut husk by the hand layup technique. The coir extracted from the husk has woody parts stuck with it and was cleaned manually by crushing it gently. Finally, the coir was cleaned with water and thoroughly dried. Further, the coir was treated with 5% NaOH solution and cleaned using distilled water to alter its surface to ensure the bonding of the coir with the polymer matrix.[40] Finally, it was perfectly dried.

A chopped strand of glass fiber, of 15±2 microns diameter and of 20 mm to 30 mm length, was purchased from Green-Tech Traders, Coimbatore, India. The matrix material used was epoxy resin LY556, with hardener HY951, purchased from Herenba Instruments & Engineers, Ambattur, Chennai, India. The recommended amount of hardener was thoroughly mixed with the resin, and the mixture was used as a matrix material to prepare the composites. Silicon carbide to be used as filler, with the size ranging from 45 μm to 90 μm, was purchased from Ultrananotech Private Ltd., Bengaluru, India.

Preparation of composite samples

The weight fraction of reinforcement and matrix was established as per the hybridization rule. The weight fraction of two or more fiber reinforcements in the same matrix was about 0.4 wt% in previous work.[44,45] In the present work, coir and glass fiber (C/GF) were used as reinforcement in the epoxy matrix to fabricate hybrid composites. Two types of composites were fabricated with various percentages of weight fractions by the hand layup technique, followed by compression molding at room

temperature. The calculated % of volume fractions of fibers and matrix is presented in Table 1.

Samples S1, S2, S3, S4, and S5 were prepared as described below. A wax-lubricated mold of 300 × 300 × 30 mm was filled with the first layer of resin mix (resin (90%) + hardener (10%)) for approximately 1 mm and allowed to solidify partially around 40 minutes. Prior to that, the silicon carbide filler (10 wt%), with the size ranging from 45 µm to 90 µm, was added to the resin mix using a tip ultrasonicator. Then, the mixture of coir and glass fibers of calculated weight was spread all over the resin layer evenly. Similarly, another set of layers was built up, and finally, the top layer was built with a resin mix approximately 1 mm thick. Further, the mold was closed and pressure of 5 bar was applied in a hydraulic press at room temperature for 24 h. Finally, the composite was cured in an oven at 60 °C for an hour. After curing, the composites were kept under sunlight for 6 hours. The schematic arrangement of layers in the prepared composites is shown in Figure 1.

Table 1
Composition of HFRC samples

Components (wt%)	Sample 1 (S1)	Sample 2 (S2)	Sample 3 (S3)	Sample 4 (S4)	Sample 5 (S5)
Coir	0	10	20	30	40
Glass fiber	40	30	20	10	0
Epoxy	50	50	50	50	50
SiC	10	10	10	10	10

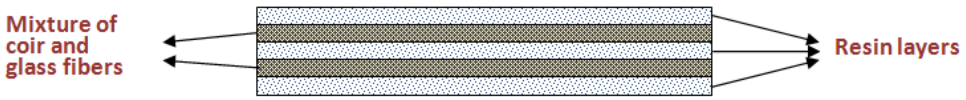

Figure 1: Schematic arrangement of layers in composite samples

Mechanical tests

Mechanical tests were conducted according to the appropriate ASTM standards. The fabricated composite plates were marked with appropriate dimensions and samples were cut using a profile cutter. Three specimens from each sample were tested and the average value was considered for further analysis. The powder produced during cutting was collected carefully and used for thermal analysis.

The samples prepared for tensile tests were cut to the size of 165 mm × 25 mm × 3 mm, to comply with the D638-10 specifications of ASTM. Three specimens from each sample were tested in a Universal Testing Machine at a uniform cross-head travel of 5 mm/min. For the flexural test, the specimens were cut to the size of 125 mm × 12.5 mm × 3 mm, according to the D790-10 specifications of ASTM, and tested in a three-point tester for 100 mm gauge length. The load was gradually increased at the rate of 5 mm/min through a load cell of 10 kN. The energy absorbed by the samples to fracture was measured by the impact test. According to the ASTM standard D256-10, samples with the dimension of 62.5 mm × 12.5 mm × 3 mm were used. The test assessed the energy absorbed by the samples during the impact of the pendulum in the impact tester.

Water absorption test

The water absorption behavior of hybrid composite samples was examined by a water absorption test conducted according to the ASTM standard D570. To measure the weight gain of the specimens, a digital scale with an accuracy of 0.001 mg was used for the experiments. The percentage of water absorption can be calculated using the equation provided below:

$$Percentage\ of\ water\ absorption\ (W\%) = \frac{W2 - W1}{W1} \quad (1)$$

where W1 represents the weight of the dry sample and W2 represents the weight of the sample after the water absorption test.

FTIR analysis

To identify the functional groups of the components of the hybrid composites, the FTIR spectra of the samples were obtained at wavelengths in the range from 4000 cm^{-1} to 400 cm^{-1} with a resolution of 8 cm^{-1} and 45 scans. A Prestige-21 FTIR spectrometer (Shimadzu, Japan) was employed to carry out FTIR analysis in Attenuated Total Reflectance (ATR) mode. A zinc selenide prism was used in the ATR accessory. The spectra were recorded after background subtraction, baseline correction, and normalization.

Thermogravimetric analysis

The thermal stability of the hybrid composite samples was tested by thermogravimetric analysis using an EXSTAR/6300 Thermogravimetric Analyser (Seiko Instruments Inc., Japan). The detailed analysis was performed under a nitrogen gas environment. The weight of the sample, taken for this analysis ranged from 10 mg to 15 mg. The composite sample was placed on the alumina pan and heated from 30 °C to 600 °C. The heating rate was kept at 20 °C/min. The

weight loss of the sample while increasing the temperature was measured.

XRD analysis

X-ray diffraction analysis of hybrid samples was carried out by a Shimadzu X-Ray Diffractometer (Model: XRD600, Kyoto, Japan) with Cu Kα radiation. The XRD patterns of hybrid samples were recorded in the 2θ range from 20° to 80° using the scanning speed of 1°/min with a 0.05° step size.

RESULTS AND DISCUSSION

Tensile strength and modulus of elasticity

The average tensile strength for each sample was determined by testing three specimens. Figure 2 displays the observed strengths and calculated modulus of elasticity, which showed significant variations. Sample S1 had the lowest strength – of 80.013 MPa, while S3 had the highest – of 107.87 MPa. The coir-reinforced composite (with no GF addition) and the GF reinforced composite (with no coir fiber addition) had weaker tensile strengths, compared to all hybrid composite samples. S3, which had equal amounts of coir and GF, had the highest strength, as observed in a similar analysis of a hybrid composite made of sisal and snake grass fibers in an epoxy matrix. It can be concluded that the addition of coir results in a higher increase in tensile strength than glass fiber. The moduli calculated followed a similar trend, with S3 having the highest modulus and S1 having the lowest. S6 had a higher modulus of elasticity than S1, but lower than that of S3. Although S4 and S5 had similar modulus of elasticity, their tensile strengths differed significantly.

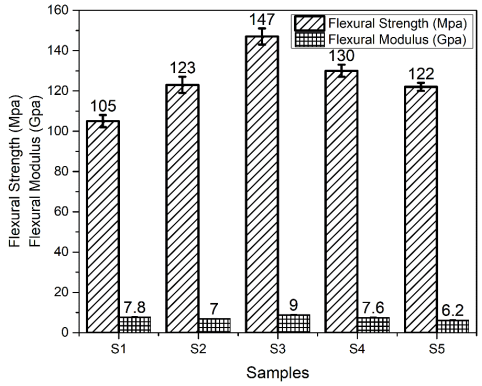

Figure 2: Tensile strengths and modulus of elasticity of hybrid composite samples

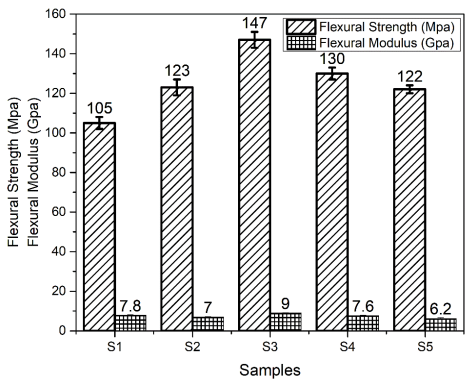

Figure 3: Flexural strengths and modulus of hybrid composite samples

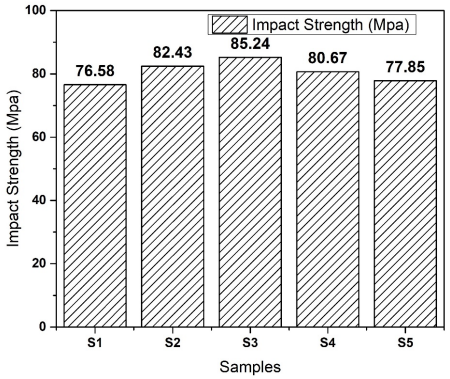

Figure 4: Impact strengths of the hybrid composite samples

Flexural strength and modulus

The flexural behaviors of the fabricated specimens were graphically presented in Figure 3. Similarly to the tensile behavior, the maximum and minimum flexural strength was found to be 146.67 MPa and 104.786 MPa for samples S3 and S1, respectively, and the corresponding moduli were 8.97 GPa and 7.84 GPa, respectively. The range of flexural strength is vast compared to the range of tensile strength obtained. It is evident that the addition of glass fiber greatly increased the flexural strength up to 20% of volume fraction. The addition of coir above the amount of GF reduced the flexural strength. The flexural

moduli behaved according to the same pattern as the tensile moduli. It depicts that the flexural modulus for every sample was almost double that of tensile modulus. This means the samples have higher bending strength than the strength in tension. Sample S6 showed an average of 125.95 MPa and the corresponding modulus was 7.723 GPa.

Impact strength

The impact strength of the specimens prepared showed notable variations due to the changes in the volume fraction of fibers, and is graphically represented in Figure 4. Similarly to the behavior pattern of tensile strength and flexural strength, S3 had the highest impact strength – of 85.24 kJ/m^2 and the lowest strength was recorded for S1. Sample S6 had an intermediate strength – of about 79.34 kJ/m^2.

The mechanical tests of the prepared samples proved that sample S3, which has an equal volume fraction of coir and glass fibers, has good strength in all the aspects examined in this study. This may be due to the effective transfer of the loads applied on the sample. Due to good bonding of the epoxy polymer with coir and glass fibers, the applied load was distributed effectively to the fibers, which improved the strength of the sample. Another sample, S6, which has a layer of coir and a layer of glass fiber, showed average strength results in all the tests. This may be because of the breakage caused by poor bonding of any of the fibers with the epoxy resin. Sample S5, with coir alone, behaves almost the same as sample S1, with glass fiber alone. Also, the strength of sample S6 was slightly higher than those of S1 and S5.

Main effects plots for tensile strength, flexural strength and impact strength

The mechanical properties of coir fibers are primarily influenced by their composition: cellulose (32-50%) provides strength and rigidity, enhancing tensile strength; lignin (30-46%) adds stiffness, durability, and impact resistance, but can increase brittleness; and hemicelluloses (0.15-15%) affect water absorption, reducing mechanical strength due to their hydrophilic nature. Increasing the coir fiber content generally enhances tensile strength up to an optimal level, but excessive fiber content can cause poor dispersion and weak interfacial bonding, reducing the overall strength. Similarly, too much coir can reduce flexural strength because of inadequate stress transfer.[10] In comparison, glass fibers enhance the tensile strength and modulus of composites significantly, as higher fiber content improves the load-bearing capacity and stress transfer between the fibers and the matrix. Glass fibers also provide greater resistance to bending stresses, thus increasing flexural strength. However, while increasing glass fiber content initially improves impact strength, excessive content can lead to brittleness, reducing the material's ability to absorb impact energy. Additionally, increasing glass fiber content typically reduces elongation at break, making the composite stiffer and less ductile.[23]

Figure 5 clearly shows that the mechanical performance of these hybrid composites will depend on the balance between coir and glass fibers. Generally, as the percentage of glass fibers increases, you can expect improved tensile and compression strength, while the impact resistance may benefit from moderate coir content, providing flexibility and energy absorption. Optimal compositions likely involve a trade-off where both fibers contribute to a synergistic enhancement of the material's mechanical properties. Among the samples, the composite containing proportions of 20% coir and 20% glass fiber, along with 10% SiC, exhibited the highest tensile strength of approximately 100 MPa, flexural strength of 146 MPa, and impact strength of 85.4 kJ/m^2.

FTIR analysis

The FTIR spectra of hybrid composite samples are presented in Figure 6. It can be noted that all the spectra showed a band in the range of 3800 cm^{-1}-3600 cm^{-1}, corresponding to the stretching vibration of the hydroxyl group, and the range of wavelength indicates that the hybrid composites have a low number of OH groups. The analysis of FTIR spectra absorption bands and the corresponding elements in the composite are summarized in Table 2. The presence of absorption bands corresponding to epoxy resin was identified in all the samples. The existence of absorption bands characteristic of the functional groups of cellulose, hemicelluloses, and lignin in the FTIR spectra confirmed the availability of coir fiber in the hybrid composites. The absorption band around 490-500 cm^{-1} was associated with the bending vibration of Si-O. Sample 5, reinforced with coir only, does not show an absorption band at 490 cm^{-1}, confirming the absence of glass fiber. Since coir and epoxy

resin share some similar functional groups, no significant differences were found in the FTIR spectra. The absorption bands corresponding to the functional groups of raw coir and glass fiber were compared and verified with literature reports.[46,47]

Figure 5: Main effects plots for tensile strength, flexural strength and impact strength

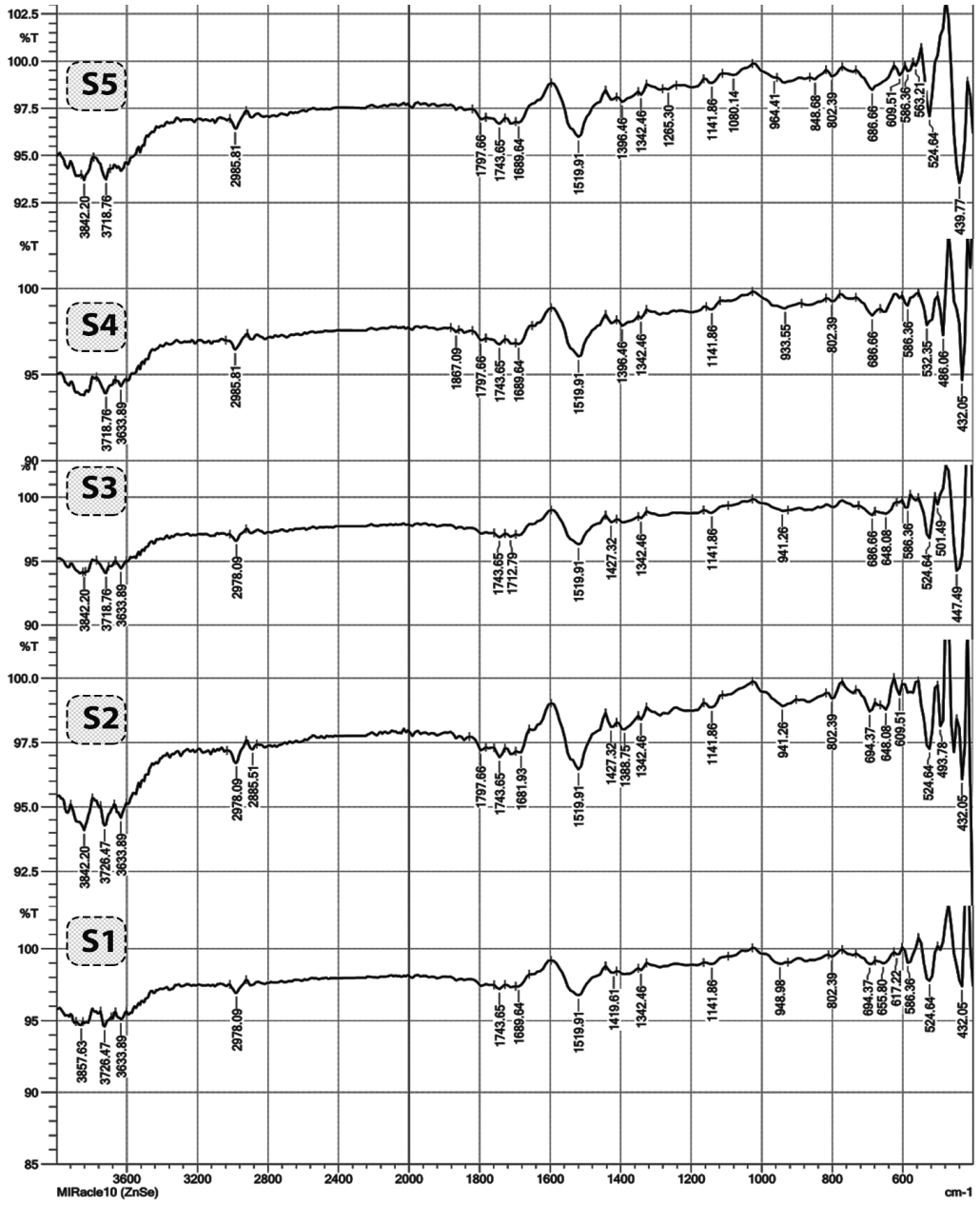

Figure 6: FTIR spectra of composite samples S1, S2, S3, S4 and S5

XRD analysis

The XRD patterns of the composite samples are shown in Figure 7. Sample 1, a composite prepared with epoxy resin and glass fiber, does not show any sharp and distinct XRD peaks, which can be attributed to the amorphous nature of the resin and glass fiber. Samples 2, 3, 4 and 5 contain coir fiber in the composite. Coir fiber is mainly composed of cellulose, along with minor content of lignin and hemicelluloses. The characteristic XRD peaks of cellulose are identified at 2θ angles of 14°, 16° and 21° in the XRD patterns of samples 2, 3, 4 and 5. The XRD analysis confirms the presence of coir fiber in the composite samples 2, 3, 4 and 5.

Table 2
Analysis of FTIR spectra absorption bands and their corresponding assignment

Wavelength (cm^{-1})	Band assignment	Interpretation
3800-3500	Bending vibration of O-H	O-H groups in cellulose present in coir; O-H groups in uncured epoxy resin; glass fiber may contain O-H groups as residual moisture
2978	Bending vibration of C-H	Methylene content in epoxy resin
1743	Stretching vibration of C=O	Hemicelluloses in coir
1700-1600	Stretching vibration of C=C	Ester in epoxy resin
1519	Stretching vibration of C=C in benzene ring	Benzene ring in epoxy resin
1400-1300	C-H bending vibration in the aromatic and aliphatic group	Aromatic and aliphatic groups in the epoxy; lignin in coir
1141	Vibrational transition of C-O bond	C-O bond in the epoxy resin structure
940-800	Out-of-plane C-H bending vibration in the aromatic ring and epoxide ring vibration	Aromatic ring in epoxy resin
750-450	Bending vibration of Si-O	Si-O bonds in glass fiber
580-460	Characteristic frequency of certain functional groups	The presence of $C_6H_4X_2$, where X may represent any functional group in the composite

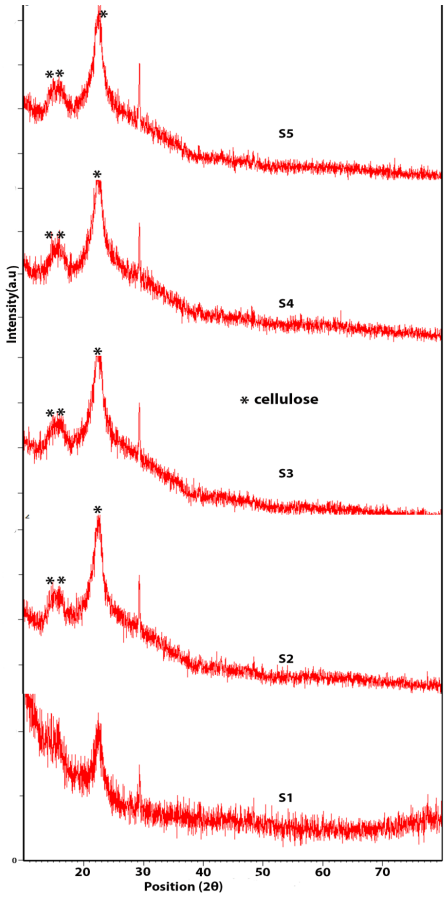

Figure 7: XRD patterns of composite samples 1, 2, 3, 4 and 5

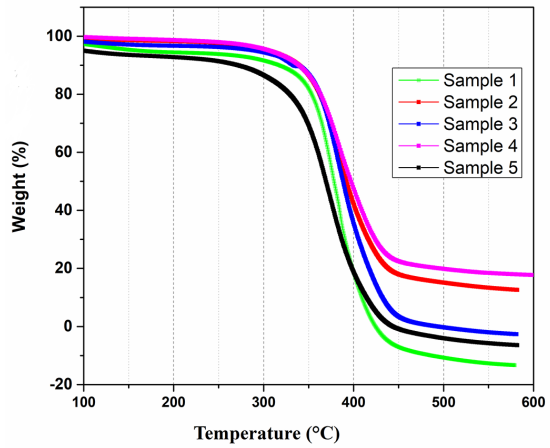

Figure 8: TGA curves of composite samples 1, 2, 3, 4 and 5

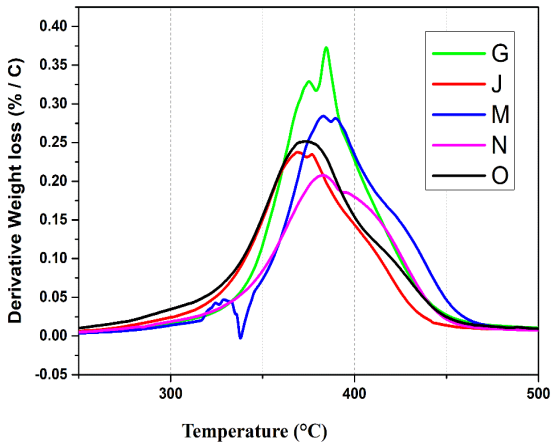

Figure 9: DTG curves of composite samples 1, 2, 3, 4 and 5

Table 3
Water absorption properties of composite samples 1, 2, 3, 4 and 5

Sample **n**umber	Immersion **t**ime (**h**)	Weight before **i**mmersion (**k**g)	Weight after **i**mmersion (**k**g)	% Weight **g**ain
1	120	0.110	0.134	24
2	120	0.105	0.124	19
3	120	0.112	0.120	8
4	120	0.106	0.144	38
5	120	0.110	0.132	23

Thermogravimetric analysis

The TGA curves of all the composite samples are shown in Figure 8. As observed from the thermograms, the curves show three distinct regions. The first region occurs as a horizontal line, with a minimum weight around the temperature range of 100-300 °C. This initial weight loss is due to the evaporation of volatile organic material and moisture content from the coir and glass fibers. Significant weight loss is observed in the temperature range of 300-450 °C. The major weight loss is associated with the decomposition of hemicelluloses, cellulose, and glass fiber. Typically, glass fiber is stable up to their glass transition temperature (Tg), but above the Tg temperature, it starts degrading.

Sample 1, prepared only with glass fiber and epoxy resin, shows a major weight loss between 350 °C and 400 °C. The hybrid composite samples 2, 3, 4, and sample 5 show thermal stability up to a temperature of around 450 °C. The higher thermal stability of these hybrid composites may be attributed to the presence of lignin in the coir. Lignin, a complex polymer in the coir, degrades at a temperature around 400-450 °C. Compared to samples 1 and 5, hybrid composite samples 2, 3, and 4 show more residues, which can be ascribed to the combined residues produced by coir fiber and glass fiber.

Wettability analysis

The impact of different compositions of natural and synthetic fibers on the water absorption property is illustrated in Table 3. By referring to Table 3, it is evident that an increase in the amount of glass fiber leads to an increased weight gain after water immersion. This can be explained by the fact that an increase in fiber content causes more micro voids to form in the matrix resin. As a result, samples 1 and 2 with 40% and 30% glass fiber exhibit greater weight gain percentages, *i.e.* 24% and 19%, respectively. In addition to that, Table 3 shows that increasing the coir fiber content also increases the wettability of the hybrid composite. The coir fibers are natural fibers, with a high concentration of hydroxyl groups, resulting in their strong water absorption ability. This leads to increased water absorption in hybrid composites. Sample 4 of the hybrid composite contains 30% coir weight percentage and showed a water weight gain percentage of 38%. Sample 5 contains 40% coir

weight percentage and showed a water weight gain percentage of 23%. Out of all the hybrid composites, the one made with 20% coir and 20% glass fiber composite had the best water absorption resistance.

CONCLUSION

In the current study, three hybrid composite samples (S2, S3, and S4) were produced, varying the proportion of coir fiber and glass fiber within the epoxy resin. The mechanical parameters, namely tensile strength, flexural strength, and impact strength, were assessed in accordance with the ASTM standards. The findings indicate that sample 3 exhibited the best tensile strength – of 100 MPa, flexural strength – of 146 MPa, and impact strength – of 85 kJ/m^2. The results of the water absorption test indicate that composite S3 demonstrated a water absorption rate of just 8%, which is significantly lower than the water absorption rates observed in the other two hybrid composites. This suggests that composite S3 exhibits greater water resistance properties compared to the other composites. The TGA results indicated that the hybrid composites exhibited superior thermal stability in comparison with the glass fiber reinforced composite. The presence of coir fiber in composite samples 2, 3, 4, and 5 was confirmed by the XRD and FTIR analyses. The findings suggest that the prepared hybrid composites have the potential to be employed in applications related to structural construction panels.

REFERENCES

[1] G. C. Jacob, J. M. Starbuck, J. F. Fellers, S. Simunovic and R. G. Boeman, *J. Appl. Polym. Sci.*, **94**, 296 (2004), https://doi.org/10.1002/app.20901

[2] V. Fiore, G. Di Bella and A. Valenza, *Mater. Des.*, **32**, 2091 (2011), https://doi.org/10.1016/j.matdes.2010.11.043

[3] A. Ahmed and L. Wei, *Rev. Adv. Mater. Sci.*, **40**, 127 (2015)

[4] A. Farokhi Nejad, M. Y. Bin Salim, S. S. Rahimian Koloor, S. Petrik, M. Y. Yahya *et al.*, *Polymers*, **13**, 3400 (2021), https://doi.org/10.3390/polym13193400

[5] A. R. De Azevedo, A. S. Cruz, M. T. Marvila, L. B. D. Oliveira, S. N. Monteiro *et al.*, *Polymers*, **13**, 2493 (2021), https://doi.org/10.3390/ polym13152493

[6] D. K. Rajak, D. D. Pagar, P. L. Menezes and E. Linul, *Polymers*, **11**, 1667 (2019), https://doi.org/10.3390/polym11101667

[7] A. Al Nouss, P. Parthasarathy, M. Shahbaz, T. Al-Ansari and H. Mackey, *Appl. Energ.*, **261**, 114350 (2020), https://doi.org/10.1016/j.apenergy.2020.114885

[8] R. Siakeng, *Express Polym. Lett.*, **14**, 717 (2020), https://doi.org/10.3144/expresspolymlett.2020.59

[9] S. K. Saw, G. Sarkhel and A. Choudhury, *J. Appl. Polym. Sci.*, **125**, 3038 (2012)

[10] A. G. Adeniyi, D. V. Onifade, J. O. Ighalo and A. S. Adeoye, *Compos. B Eng.*, **176**, 107305 (2019), https://doi.org/10.1016/j.compositesb.2019.107305

[11] P. Vinod, A. B. Bhaskar, G. Sreelekshmy Pillai and S. Sreehari, *J. Nat. Fibers*, **6**, 278 (2009), https://doi.org/10.34218/IJARET.11.7.2020.0 20

[12] M. Sayida, S. Evangeline, A. Vijayan and M. Girish, *J. Nat. Fibers*, **46**, 2288 (2022), https://doi.org/10.1080/15440478.2020.1808146

[13] M. Prambauer, C. Wendeler, J. Weitzenböck and C. Burgstaller, *Geotext. Geomembr.*, **47**, 48 (2019), https://doi.org/10.1016/j.geotexmem.2018.09.006

[14] V. Salazar, A. L. Leão, D. Rosa and J. Gomez, *J. Polym. Environ.*, **19**, 677 (2011)

[15] M. R. Ketabchi, M. E. Hoque and M. K. Siddiqui, "Manufacturing of Natural Fibre Reinforced Polymer Composites", Springer, Berlin, 2015, pp. 125–138

[16] K. M. F. Hasan, P. G. Horváth and T. Alpár, *Polymers*, **12**, 1072 (2020), https://doi.org/10.3390/polym12051072

[17] R. Siakeng, M. Jawaid, H. Ariffin and S. Sapuan, *Polym. Compos.*, **40**, 2000 (2019), https://doi.org/10.1002/pc.24978

[18] K. Venkatesan and G. B. Bhaskar, *Fibers Polym.*, **21**, 1523 (2020), https://doi.org/10.1007/s12221-020-9532-5

[19] S. Sathees Kumar, *Fibers Polym.*, **21**, 1508 (2020), https://doi.org/10.1007/s12221-020-9853-4

[20] M. T. Zafar, S. N. Maiti and A. K. Ghosh, *Fibers Polym.*, **17**, 266 (2016), https://doi.org/10.1007/s12221-016-5781-8

[21] Y. Liu, B. Sun, X. Zheng, L. Yu and J. Li, *Bioresour. Technol.*, **247**, 859 (2018), https://doi.org/10.1016/j.biortech.2017.08.059

[22] M. N. Akhtar, A. Bakar Sulong, M. K. Fadzly Radzi, N. F. Ismail, M. R. Raza *et al.*, *Prog. Nat. Sci. Mater. Int.*, **26**, 657 (2016), https://doi.org/10.1016/j.pnsc.2016.12.004

[23] K. M. Faridul Hasan, P. G. Horváth, Z. Kóczán and T. Alpár, *Sci. Rep.*, **11**, 3618 (2021), https://doi.org/10.1038/s41598-021-83140-0

[24] J. Qureshi, *Fibers*, **10**, 27 (2022), https://doi.org/10.3390/fib10030027

[25] I. S. Abbood, S. A. Odaa, K. F. Hasan and M. A. Jasim, *Mater. Today Proc.*, **43**, 1003 (2021), https://doi.org/10.1016/j.matpr.2020.07.636

[26] A. Czapla, M. Ganesapillai and J. Drewnowski, *Processes*, **9**, 2238 (2021), https://doi.org/10.3390/pr9122238

[27] C. Bedon and C. Louter, *Am. J. Eng. Appl. Sci.*, **9**, 713 (2016), https://doi.org/10.3844/ajeassp.2016.680.691

[28] Z. Wu, X. Wang, X. Zhao and M. Noori, *Int. J. Sustain. Mater. Struct. Syst.*, **1**, 201 (2014)
[29] L. C. Hollaway, *Constr. Build. Mater.*, **24**, 2419 (2010), https://doi.org/10.1016/j.conbuildmat.2010.04.062
[30] PT Intec Persada, available online: https://intecpersada.com/fibregutter/ (accessed on 17 May 2022)
[31] D. K. Rajak, D. D. Pagar, P. L. Menezes and E. Linul, *Polymers*, **11**, 1667 (2019), https://doi.org/10.3390/polym11101667
[32] A. Zaman, S. A. Gutub and M. A. Wafa, *J. Reinf. Plast. Compos.*, **32**, 1966 (2013), https://doi.org/10.1007/978-3-030-81162-4_55
[33] T. P. Sathishkumar, S. Satheeshkumar and J. Naveen, *J. Reinf. Plast. Compos.*, **33**, 1258 (2014), https://doi.org/10.1177/0731684414530790
[34] M. M. Y. Zaghloul, K. Steel, M. Veidt and M. T. Heitzmann, *J. Reinf. Plast. Compos.*, **41**, 215 (2022), https://doi.org/10.1007/s12221-024-00671-9
[35] S. Manteghi, Z. Mahboob, Z. Fawaz, H. Bougherara and J. Mech, *Behav. Biomed. Mater.*, **65**, 306 (2017), https://doi.org/10.1016/j.jmbbm.2016.08.035
[36] N. Ramadan, I. Taha, R. Hammouda and M. H. Abdellatif, *Polym. Compos.*, **25**, 333 (2017), https://doi.org/10.1177/096739111702500503
[37] R. B. Yusoff, H. Takagi and A. N. Nakagaito, *Ind. Crop. Prod.*, **94**, 562 (2016), https://doi.org/10.1016/j.indcrop.2016.09.017
[38] S. Nunna, P. R. Chandra and S. Shrivastava, *J. Reinf. Plast. Compos.*, **31**, 759 (2012), https://doi.org/10.1177/0731684412444325
[39] C. Dong, *J. Reinf. Plast. Compos.*, **38**, 910 (2019), https://doi.org/10.1177/0731684419856686
[40] M. Vijayakumar, K. Kumaresan, R. Gopal, S. D. Vetrivel and V. Vijayan, *New Mater. Electrochem. Syst.*, **24**, 120 (2021), https://doi.org/10.14447/jnmes.v24i2.a09
[41] R. V. Da Silva, H. Voltz, A. I. Filho, M. Xavier Milagre and C. de S Carvalho Machado, *J. Compos. Mater.*, **55**, 717 (2021), https://doi.org/10.1177/0021998320957725
[42] T. Sadik, S. Muthuraman, M. Sivaraj, K. Negash and R. Balamurugan, *Adv. Mater. Sci. Eng.*, 9882769 (2022), https://doi.org/10.1155/2022/9882769
[43] K. M. F. Hasan, P. G. Horváth and Z. Kóczán, *Sci. Rep.*, **11**, 3618 (2021), https://doi.org/10.1038/s41598-021-83140-0
[44] M. K. Gupta, M. Ramesh and S. Thomas, *Polym. Compos.*, **42**, 4981 (2021), https://doi.org/10.1002/pc.26244
[45] M. Z. R. Khan, S. K. Srivastava and M. Gupta, *J. Reinf. Plast. Compos.*, **37**, 1435 (2018), https://doi.org/10.1177/0731684418799528
[46] A. S. Asha and A. S. M. Raja, *Int. J. Sci. Eng. Res.*, **10**, 379 (2019)
[47] J. Rouhi, S. Pourhashem and A. Ahmadi, *J. Mater. Sci. Res.*, **4**, 1 (2015)